Available online at www.sciencedirect.com

SciVerse ScienceDirect

journal homepage: www.elsevier.com/locate/he

Numerical study of spontaneous ignition in pressurized hydrogen release through a length of tube with local contraction

*B.P. Xu, J.X. Wen**

Centre for Fire and Explosion Studies, Faculty of Engineering, Kingston University, Friars Avenue, London SW15 3DW, UK

ARTICLE INFO

Article history:
Received 20 December 2011
Received in revised form
7 April 2012
Accepted 28 April 2012
Available online 10 June 2012

Keywords:
Hydrogen
Spontaneous ignition
Shock reflection
Contraction
Numerical simulation

ABSTRACT

Numerical investigations have been conducted on the effect of the internal geometry of a local contraction on the spontaneous ignition of pressurized hydrogen release through a length of tube using a 5th-order WENO scheme. A mixture-averaged multi-component approach was used for accurate calculation of molecular transport. The auto-ignition and combustion chemistry were accounted for using a 21-step kinetic scheme. It is found that a local contraction can significantly facilitate the occurrence of spontaneous ignition by producing elevated flammable mixture and enhancing turbulent mixing from shock formation, reflection and interaction. The first ignition kernel is observed upstream the contraction. It then quickly propagates along the contact interface and transits to a partially premixed flame due to the enhanced turbulent mixing. The partially premixed flames are highly distorted and overlapped with each other. Flame thickening is observed, which is due to the merge of thin flames. The numerical predictions suggested that sustained flames could develop for release pressure as low as 25 bar. For the release pressure of 18 bar, spontaneous ignition was predicted but the flame was soon quenched. To some extent this finding is consistent with Dryer et al.'s experimental observation in that the minimum release pressure required to induce a spontaneous ignition for the release through a tube with internal geometries is only 20.4 bar.

1. Introduction

As a possible next-generation energy carrier, safe transport and utilization of compressed hydrogen is of particular importance. A potential hazard of such system is high pressure hydrogen jet originating from either a pressure relief valve or a small crack in the piping of a storage vessel. Such jets are often ejected in the presence of obstacles, either impinging surfaces or turbulence inducing structures and inevitably their behaviour (including spontaneous ignition and flame propagation if ignited) is strongly subject to the influence of these surrounding obstacles. In some accidental scenarios, pressurized hydrogen releases were found to have ignited when there was no clearly identifiable ignition source [1]. The ignition can potentially lead to jet fires, rapid flame acceleration and explosions in confined areas. In a recent review by the Health and Safety Laboratory [2] on the properties and hazards of some alternative fuels, it was highlighted that "Research is required to determine the mechanisms of apparently spontaneous hydrogen ignition

* *Corresponding author.*
E-mail address: j.wen@kingston.ac.uk (J.X. Wen).

0360-3199/$ – see front matter
doi:10.1016/j.ijhydene.2012.04.150

when it leaks from highly pressurized containment and to quantify the risk of ignition occurring". The presence of obstacles/walls is also expected to affect spontaneous ignition and further complicates the underlying physics.

Although several ignition mechanisms have been postulated and examined in the literature [1,3], there still lacks clear understanding about the ignition mechanisms. Among the postulated mechanisms, the reverse Joule-Thomson effect has been ruled out while diffusion ignition has been demonstrated by both experiments [3–5] and numerical simulations [6–14] which suggested that the mechanism of the spontaneous ignition is due to shock-induced diffusion ignition. As compressed hydrogen is abruptly released into atmospheric environment, a strong shock wave forms and propagates into ambient air raising its temperature and pressure; meanwhile a rarefaction wave moves back into the compressed hydrogen reducing its temperature and pressure. The shock-heated air mixes with the cooling decompressed hydrogen at the contact region. If the temperature of the combustible mixture within the flammability limit exceeds the auto-ignition temperature, spontaneous ignition will occur after an ignition delay time.

Most previous experimental studies [3–5] focused on phenomenological observations of pressurized releases through a length of tube. According to these experimental observations, release pressure and length of release tube are two important factors affecting the occurrence of the spontaneous ignition. A higher release pressure would facilitate the occurrence of ignition by producing a higher temperature of the oxidizer, while a longer tube would provide a longer mixing time to make ignition more readily happen. Dryer et al. [3] also emphasized the importance of the internal geometry downstream of the burst disk and the multi-dimensional shock formations/reflections/interactions resulting from the rupture process of the burst disk, and postulated that both factors were responsible for significant mixing occurring at contact surface. In Dryer et al.'s experimental observation the minimum release pressure to induce an ignition for a release through a tube with internal geometries is as low as 20.4 bar.

Numerical investigations have also been attempted for both direct releases [6–8] and releases through a length of tube [9–14]. These studies successfully predicted the occurrence of the spontaneous ignition and demonstrated the capability of numerical simulations to investigate this complex phenomenon for which previous experimental studies could only provide qualitative results. Xu et al. [7] numerically investigated the effect of pressure boundary rupture rate on spontaneous ignition of direct releases using an Iris model to mimic the actual rupture process. The Iris model is used to simulate the finite opening time of the pressure boundary. It assumes the pressure boundary, which is mimicked by a thin diaphragm, ruptures linearly from the centre at a finite pre-determined rate. It was evident that the rupture process of the pressure boundary could not be considered as to be infinitely fast due to the very fast flow characteristic time scale. A finite rupture time would result in a much lower temperature of the shock-heated air compared to an infinitely fast rupture and hence greatly reduce the likelihood of the spontaneous ignition of a direct release. More recently, Wen et al. [10] carried out a detailed numerical study of compressed hydrogen releases through a length of tube taking into account the finite rupture time. It was found that the finite rupture process plays an important role in the spontaneous ignition. The finite rate rupture process produces higher-than-ideal shock velocity and significant turbulent mixing at contact region and provides additional heating to the combustible mixture via shock reflections and interactions. It was revealed that ignition is firstly initiated at highly distorted contact region by strong turbulence induced by the rupture process inside the tube and gradually evolves into a partially premixed flame along the contact region. Critical amount of shock-heated air and well developed partially premixed flames are two major factors providing potential energy to overcome the strong under-expansion following spouting from the tube exit.

All the aforementioned previous numerical studies were concerned with releases through a length of tube with constant cross-section. Inspired by Dryer et al.'s findings of the importance of the internal geometry downstream of the burst disk, numerical study of spontaneous ignition in compressed hydrogen release through a length of tube with a local contraction is conducted to investigate the effect of the internal geometry using our previously developed numerical model [10]. The local contraction is a good example of internal geometries since it will induce a contracting flow followed by an expanding flow from which strong shock reflection, interaction and focusing will develop.

2. Numerical methods

Numerical study of the spontaneous ignition in compressed hydrogen release is of particular challenge because of the substantial scale difference between diffusion and advection and the reactive flow accompanied by strong shock waves. Diffusion across the contact region is a much slower process than the fast characteristic flow time. To explicitly resolve physical diffusion at the contact region, high-order numerical schemes along with fine grid resolution are required to prevent it from being smeared by numerical diffusion. For applications involving rich shock structures, high-order WENO shock-capturing schemes are more efficient than low order total variation diminishing (TVD) schemes and can help to reduce numerical diffusion [15]. Although second-order TVD schemes were widely used in previous numerical studies of the hydrogen spontaneous ignition [6,9,13,14], preliminary numerical tests have shown that numerical diffusion resulting from second-order schemes artificially enhances the mixing at contact region and over-predicts the likelihood of spontaneous ignition.

Considering the substantial scale difference between diffusion and advection, an arbitrary Lagrangian and Eulerian (ALE) method [16] was adopted to treat convective terms separately from diffusion terms in the transport equations. Each computational time step is divided into two phases in the ALE method, i.e. a Lagrangian phase and a rezone phase. In the Lagrangian phase, a second-order Crank-Nicolson scheme is used for the diffusion terms and the terms associated with pressure wave propagation, a 3rd-order TVD Runge–Kutta method [17] is used in the rezone phase to solve the convection terms. The coupled semi-implicit equations in the

Lagrangian phase are solved by a SIMPLE type algorithm with individual equations solved by a conjugate residual method [18]. For spatial differencing, a 5th-order upwind WENO scheme [15] is used for the convection terms and the second-order central differencing scheme is used for all the other terms.

It has been shown [19] that the treatment of molecular transport is crucial to the accurate predictions in a non-premixed counterflow flame. A full multi-component formulation is known to give more accurate predictions than a mixture-averaged multi-component approach for molecular transport, but the former is much more time-consuming. Our previous study has shown that the rupture process rapidly generates a highly turbulent flow [11], implying that the underlying physics is dominated by turbulent transport rather than molecular mixing except for the very early stage of the release. Therefore the less time-consuming mixture-averaged multi-component formulation is chosen in the present study [20] for the calculation of molecular transport with consideration of thermal diffusion which is important for non-premixed hydrogen combustion. For autoignition chemistry, Saxena and Williams' detailed chemistry scheme [21] which involves 21 elementary steps among eight reactive chemical species was used. The scheme was previously validated against a wide range of pressures up to 33 bar. It also gave due consideration to third body reactions and the reaction-rate pressure dependent ''fall-off'' behaviour. To deal with the stiffness problem of the chemistry, the chemical kinetic equations were solved by a variable-coefficient ODE solver [22]. More detailed description of the numerical models and validations can be found in Wen et al. [11].

3. Problem descriptions

It was revealed in our previous study [11] that spontaneous ignition first occurs inside release tubes and gradually evolves into a partially pre-mixed flame before jetting out of tube exits. Therefore, the present study is limited to the flow inside the release tube. The computational domain is composed of a cylindrical high-pressure vessel of large diameter and a release tube with a local contraction shown in Fig. 1. The pressurized cylinder was set up to be sufficiently large to ensure that pressure drop during simulations does not exceed 3% of the initial pressure. The release tube has a diameter D of 3 mm and a length L of 6 cm. The contraction ratio is fixed to be 0.6 in this study. The distance of the local contraction to the rupture plane is chosen as 5 times of the tube diameter, which ensures the incident shock to reach a nearly constant shock velocity before it transmits into the contraction section if the finite opening time of the pressure boundary is taken into account. The width of the local contraction is set to be the tube diameter. In our previous study [11] it was found that the rupture process of the initial pressure boundary is crucial to the spontaneous ignition. An Iris model [23] is used to simulate the rupture process of the pressure boundary. It assumes that the pressure boundary, which is mimicked by a thin diaphragm with a thickness of 0.1 mm placed at the left plane of the release tube in the simulations, ruptures linearly from the centre at a finite pre-determined rate as simulations start. According to our previous study [11] the rupture time, which is the time for a full bore opening of the thin diaphragm depends on its material, thickness and diameter as well as the rupture pressure. For the current problem set up the rupture time is estimated to be within a range of 5–30 μs. It was also revealed [11] that although the shock velocity finally stabilizes at approximately the same value following the release at different rupture rates, the longer the rupture time, the slower the increase rate of the shock velocity. The effect of rupture time was previously investigated by the authors [7] and not in the scope of the present study. In order to obtain a fast increase rate of the shock velocity, the rupture time is fixed as 5 μs for all the cases studied here. Three release pressures of 50 bar, 25 bar, 18 bar, which are not sufficiently high to produce a spontaneous ignition for a tube of a constant cross-section, are considered in this study. According to Dryer et al.'s findings, a release pressure of only 18 bar would not produce spontaneous ignition for any internal geometries.

All the simulations were started from still conditions with the tube filled with ambient air and the pressurized cylinder region with pure pressurized hydrogen separated by a thin diaphragm with a thickness of 0.1 mm. All the solid surfaces (e.g. walls) were assumed to be non-slip and adiabatic. Non-uniform grids were applied to the regions of pressurized cylinder and uniform grids to the tube region. Since flame is first initiated at the thin contact region, a very fine grid resolution is required there to resolve the species profiles in the ignited flame. According to our previous study [11] a 15 μm mesh size is sufficient to resolve the species profiles hence used in this study. The non-uniform grids were clustered around the two ends of the tube and the grid sizes range from 15 μm–150 μm inside the region of pressurized cylinder. The total grid points are then approximately two millions in the current simulations. The key parameters of the computed release scenarios are summarized in Table 1.

4. Results and analysis

It was revealed in our previous study [11] that a curvilinear incident shock is quickly generated and reflected from the tube wall. The reflected shock converges at the axis of symmetry creating shock focusing. The repeating processes of shock reflection and focusing create an intermittent flow pattern of circular and central flows causing a tongue-shaped contact region (see Fig. 3(a)). Following rupture, the shock velocity reflecting the strength of the incident shock gradually

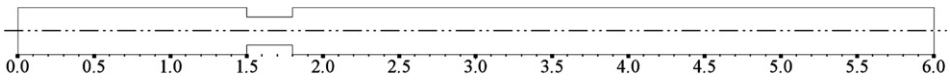

Fig. 1 – Schematic of the release tube with local contraction (length unit in cm).

Table 1 – Computational details.

Parameters	Values
Rupture time (μs)	5
Release pressure (bar)	50, 25, 18
Initial temperature (K)	293
Diameter of tube (mm)	3
Length of tube (mm)	60
Contraction ratio	0.6
Thickness of film (mm)	0.1
Minimum grid spacing (μm)	15

reaches maximum and then slowly decreases. For the current release conditions, the maximum shock velocity is reached approximately at a distance 5 times the tube diameter downstream the rupture plane, i.e. the location of the local contraction. Figs. 2 and 3 show a close-up of the flow development at the local contraction using the predicted contours of pressure, axial velocity, temperature, and hydrogen mass fraction for the case of 50 bar. The incident shock reaches the contraction at roughly $t = 13$ μs (Fig. 2(a)) and the flow behind it shows a turbulent behaviour due to the intermittent flow. The outer part of the incident shock is reflected from the left vertical wall of the contraction while the central part of it is transmitted into the contraction tube. A curvilinear reflected shock is generated at $t = 14$ μs (Fig. 2(b)) receding towards the rupture plane. Behind the reflected shock the incident flow is quickly decelerated accompanied by an elevated temperature. The curvilinear reflected shock converges and reflects from the axis of symmetry creating a high-speed jet flow inside the contraction section at $t = 15$ μs (Fig. 2(c)). The tip of the contact region is narrowed and penetrates towards the planar transmitted shock.

As the transmitted shock leaves from the contraction section, it diffracts into a curvilinear shock which will be reflected from the tube wall at $t = 16$ μs (Fig. 2(d)). The reflected shock converges at the axis creating another high speed jet. As the reflected shock interacts with the leading shock, an annular Mach stem develops along the tube wall at $t = 18$ μs (Fig. 2(f)) in the form of a von Neumann Mach reflection [24]. The shock reflections, focusing and interactions create a highly turbulent flow significantly distorting the contact region and enhancing its mixing. The fast turbulent mixing leads to the creation of a partially premixed layer between hydrogen and shock-heated air. An ignition kernel is firstly observed at $t = 14$ μs (Fig. 3(b)) at the contact region near the left edge of the contraction section where temperature of the flammable mixture is highest and then tends to propagate along the interface. At $t = 15$ μs (Fig. 3(c)) another ignition kernel emerges at the tube wall behind the reflected shock. Two flames evolving from the ignition kernel are connected to be a partially premixed flame at $t = 17$ μs (Fig. 3(e)). It is also evident that as the frontal part of the flame convects out of the contraction tube local flame extinction occurs due to the strong flow divergence (Fig. 3(f–g)).

Fig. 4 shows the predicted contours of pressure and axial velocity at a time interval of 4 μs starting from 22 μs for the case of 50 bar. As the leading shock wave propagates downstream the contraction section, a strong Mach disk gradually forms at the location of $x = 2$ cm (see Fig. 4(a)). Ahead of the Mach disk the flow is abruptly decelerated to be subsonic and the pressure is recovered, while an annular supersonic flow develops along the tube wall. Inside the annular flow local shocklets form due to the supersonic flow creating an intermittent flow pattern and the annular flow gradually touches the axis. It is also evident from Fig. 4(e–f) that the annular flow

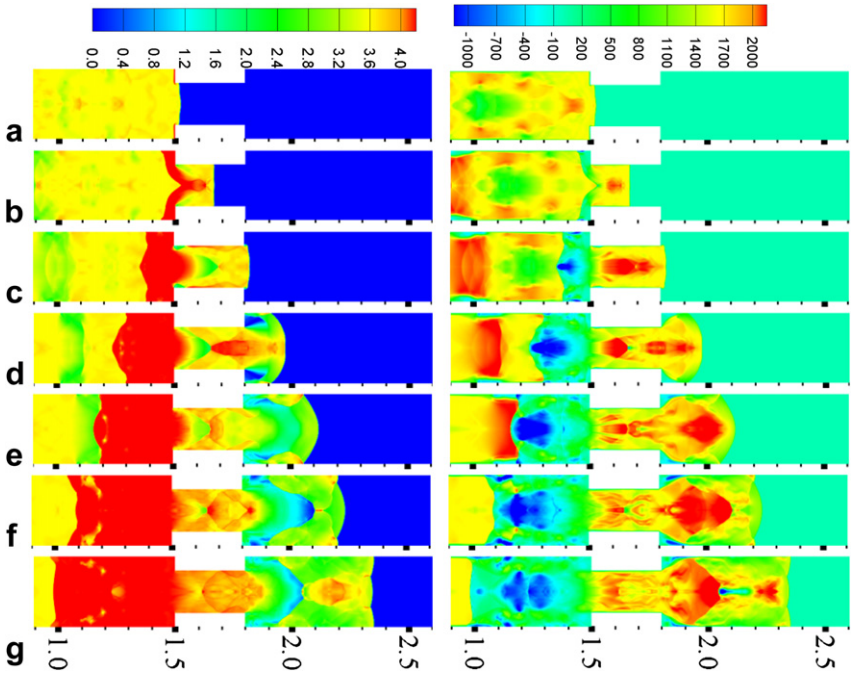

Fig. 2 – Predicted contours of Logarithm of pressure (bar) in the left column and axial velocity (m/s) in the right column at a time interval of 1 μs starting from 13 μs for the case of 50 bar (length unit in cm).

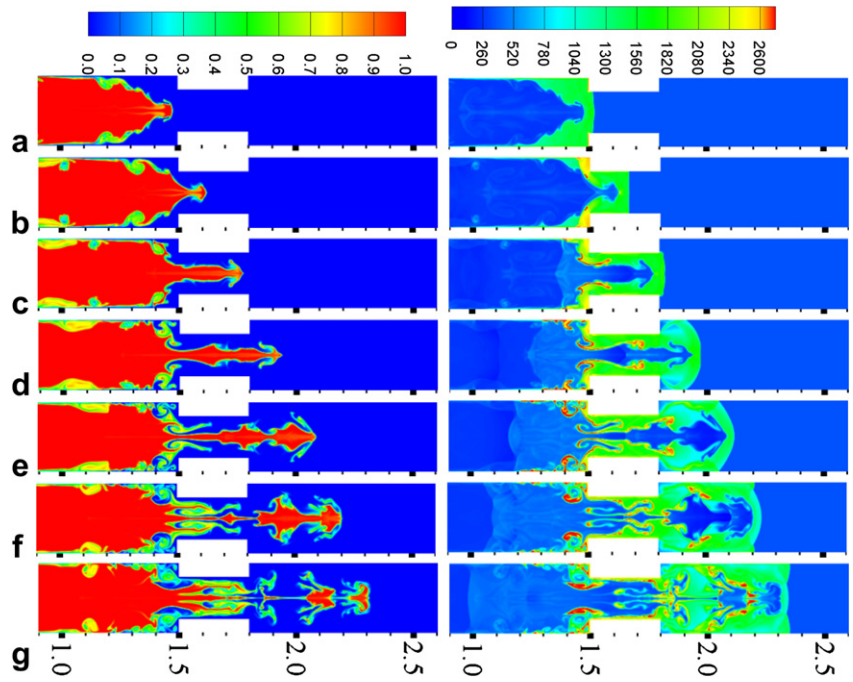

Fig. 3 – Predicted contours of Logarithm of hydrogen mass fraction in the left column and temperature (K) in the right column at a time interval of 1 μs starting from 13 μs for the case of 50 bar (length unit in cm).

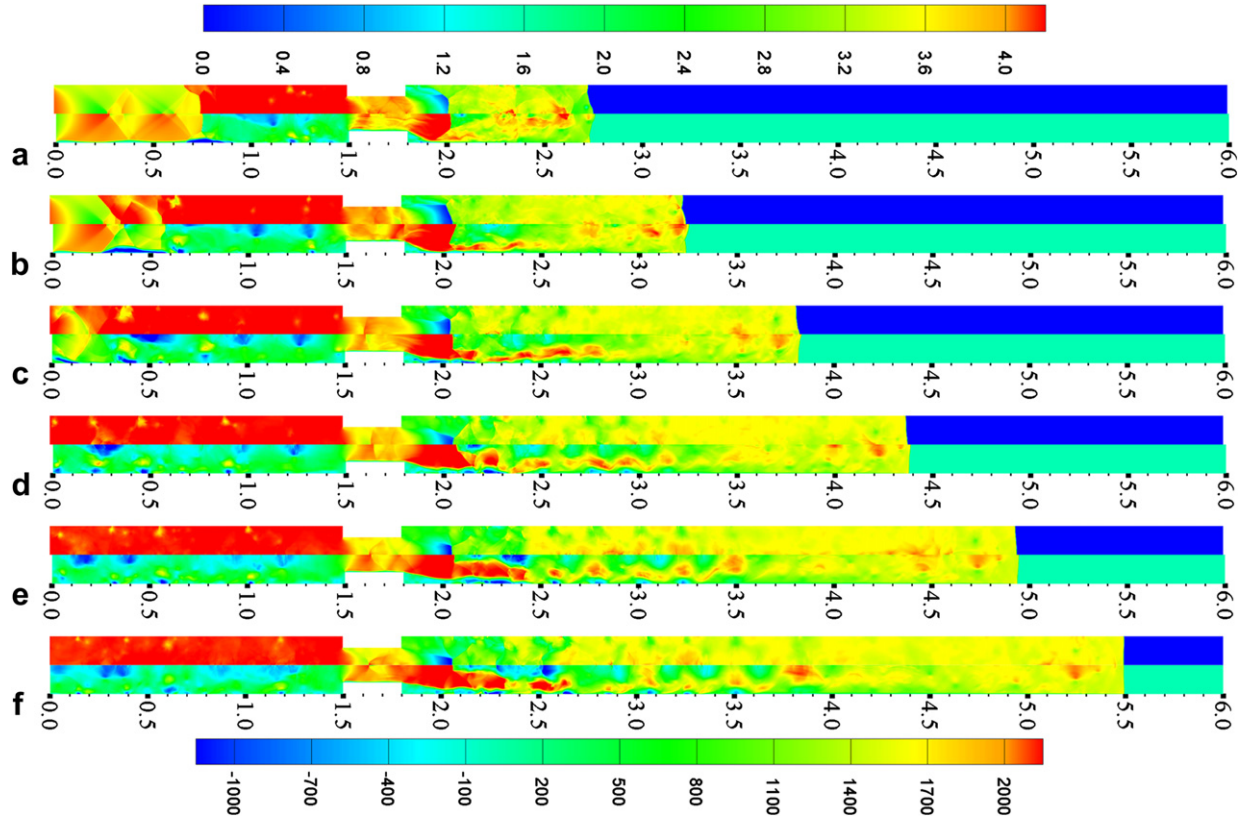

Fig. 4 – Predicted contours of Logarithm of pressure (bar) and axial velocity (m/s) at a time interval of 4 μs starting from 22 μs for the case of 50 bar (length unit in cm). (Pressure is shown in the upper half of each frame; while axial velocity is shown in the lower half of each frame.)

also induces a reverse flow at the tube axis downstream the Mach disk. Due to the flow development, significant turbulence is created downstream the contraction.

Fig. 5 shows the predicted contours of OH mass fraction and hydrogen mass fraction at a time interval of 4 μs starting from 22 μs for the case of 50 bar. As the contact region convects downstream the contraction, it is highly distorted by the turbulent flow and its front tip penetrates into the shock-heated air. Meanwhile significant amount of flammable mixture quickly forms due to the turbulent enhanced mixing. At the front of the mixing region, low hydrogen concentration mixing "islands" surrounded by shock-heated air are observed. Although the ignition kernels are initiated at the thin contact region, partially premixed flames quickly develop due to the fast turbulent enhanced mixing. The flames located close to the low flammability limit due to high mixing temperature are quickly extended. Majority of the flames are located at the front mixing regions overlapping with each other. Flame thickening is observed due to the merge of thin flames. Apart from the front flames, flames are also observed at the tube wall and the recirculation zone behind the backward-facing step.

Figs. 6 and 7 respectively show scattered plots of temperature and OH radical mass fraction versus mixture fraction at every computational cell centres for the case of 50 bar. The mixture fraction is defined by

$$f = \frac{\phi Y_{H_2} - Y_{O_2} + Y_{O_2,inf}}{\phi Y_{H_2,inf} + Y_{O_2,inf}} \quad (1)$$

where the mass ratio of oxygen to hydrogen at stoichiometry $\phi = 8$, Y_{H_2} and Y_{O_2} are mass fractions of hydrogen and oxygen respectively, $Y_{O_2,inf} = 0.23$ and $Y_{H_2,inf} = 1.0$ are mass fractions at infinity. The stoichiometric mixture fraction is therefore $f_{st} = 0.028$, while for pure air and pure hydrogen the mixture fraction is equal to 0.0 and 1.0 respectively. At $t = 12$ μs, the incident shock is just about to reach the contraction. Temperature dependence on mixture fraction shows large scatter indicating multi-dimensional turbulent behaviour of the release flow. The minimum temperature is 145 K occurring at $f = 1.0$ due to the cooling effect from the initial diffraction waves, while the maximum temperature is 1641 K occurring at $f = 0.0$ for shock-heated air inside the boundary layer. Temperature increases with a decreasing mixture fraction due to the heat exchange between shock-heated air and hydrogen via mixing. The maximum temperature at the stoichiometric mixture fraction is approximately 1000 K at which the ignition induction time is in the order of 100 μs [10] prohibiting ignition to occur inside the tube. At $t = 14$ μs, the incident shock reflects from the left vertical wall further raising temperature behind the reflected shock. At this instance, the maximum temperature of the unburned mixture at the stoichiometric mixture fraction is roughly 1500 K at which the ignition induction time is only in the order of 1 μs quickly inducing an ignition. The scatter of OH mass fraction at $t = 14$ μs is sparse indicting the initial ignition taking place at a small kernel. The ignition kernel has a significant thickness in the mixture fraction space spanning from $f = 0.0$ to $f = 0.08$ and the reaction rate peaks at a mixture fraction $f_{mr} = 0.025$ called most reactive mixture fraction slightly deviating from the stoichiometric mixture fraction $f_{st} = 0.028$. After the ignition, the ignition kernels are quickly extended along the interface, which is evident from the increasingly dense scattered distribution of OH mass fraction. Temperature dependence on mixture fraction shows large scatter from $t = 16$ μs to $t = 32$ μs during the flame spreading. It is evident from Fig. 6(f) that most of temperature scatter points cluster around equilibrium values indicating that the flames almost spread over all the interfaces between hydrogen and shock-

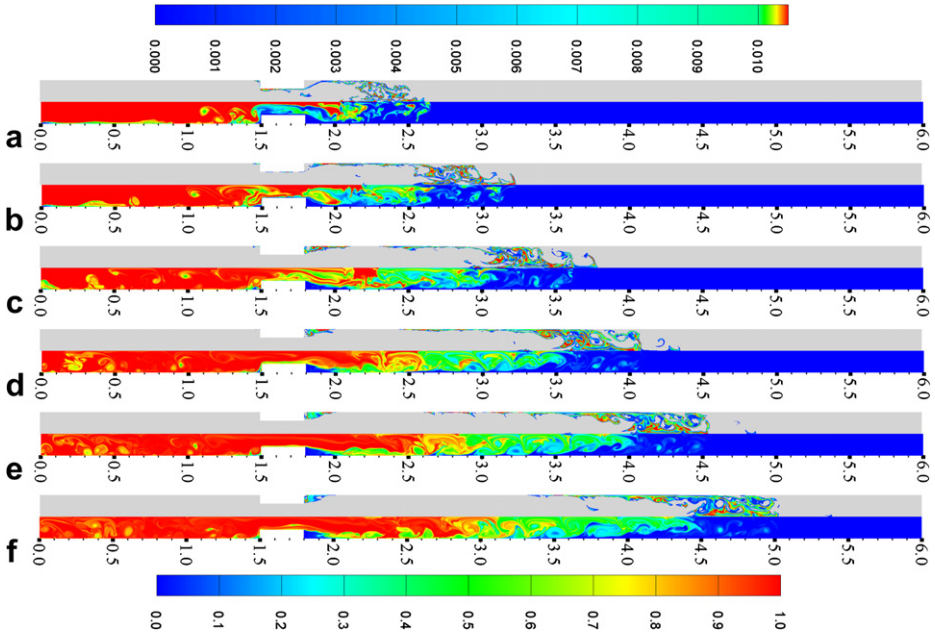

Fig. 5 – Predicted contours of OH mass fraction and hydrogen mass fraction at a time interval of 4 μs starting from 22 μs for the case of 50 bar (length unit in cm). (OH mass fraction is shown in the upper half of each frame; while mass fraction is shown in the lower half of each frame.)

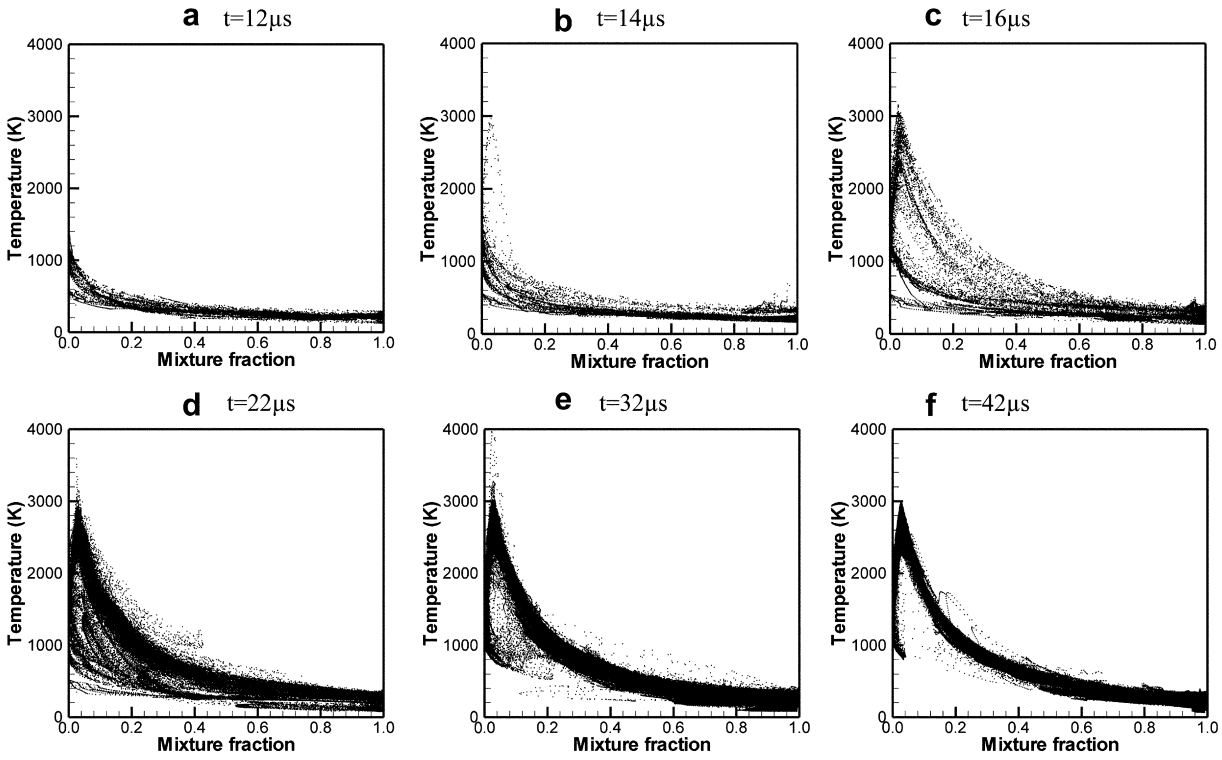

Fig. 6 – Scattered plots of temperature versus mixture fraction for the case of 50 bar at different instance.

heated air. At $t = 42$ μs, OH radical mass fraction still show large scatter owing to the different local flow conditions resulting from the highly turbulent flow.

Fig. 8 shows the maximum temperature versus release time. For the cases of 50 bar release, the maximum temperature jumps to 1046 K at $t = 0.2$ μs after the rupture due to the shock heating and then drops to 624 K at $t = 2.3$ μs due to the flow divergence. After $t = 2.3$ μs it quickly increases again due to the shock reflection. Two spikes at $t = 6.6$ μs and 8.3 μs are caused by shock focusing. For the case with a constant

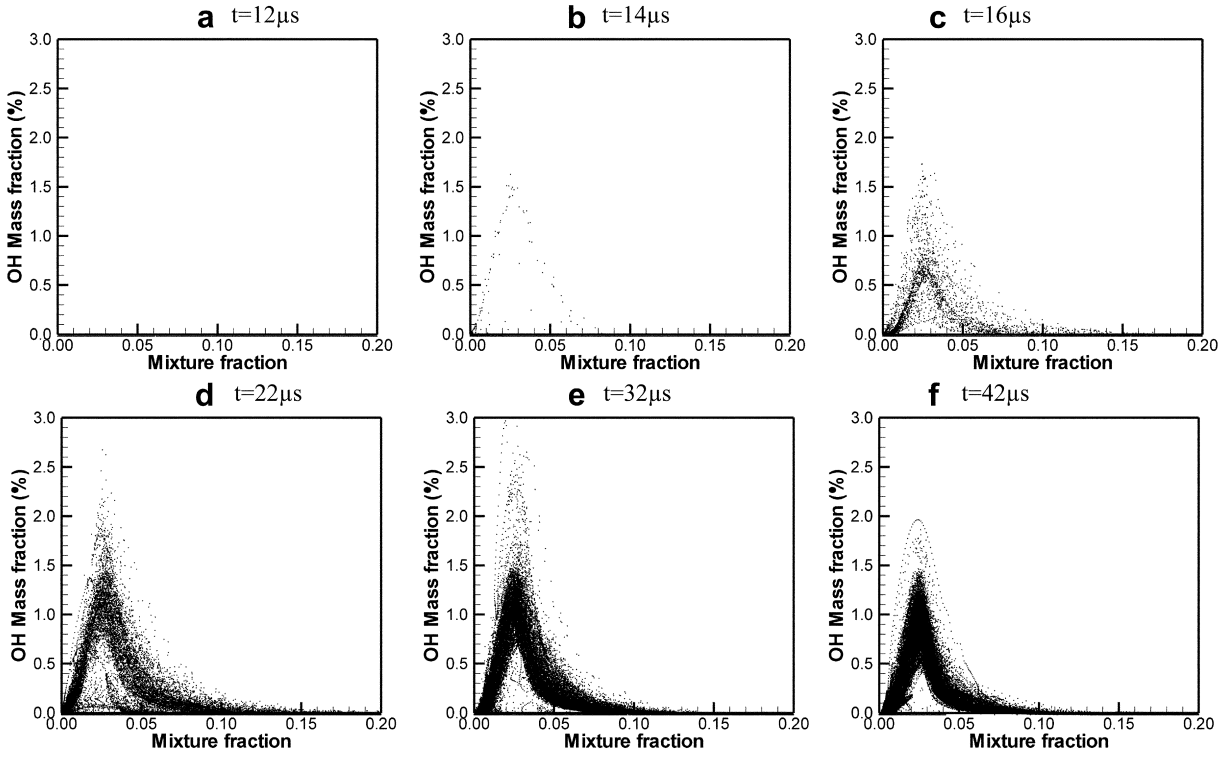

Fig. 7 – Scattered plots of OH radical mass fraction versus mixture fraction for the case of 50 bar at different instance.

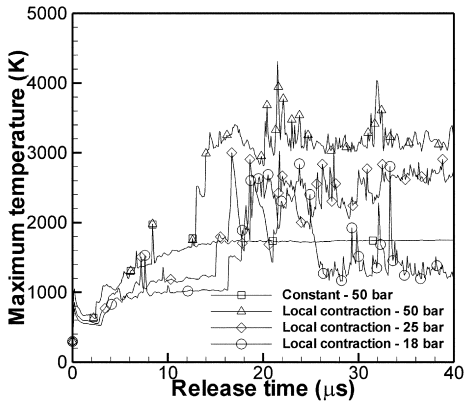

Fig. 8 – Maximum temperature versus release time.

cross-section, it finally stabilizes a value of 1653 K from $t = 13$ μs and no ignition occurs. For the case with a local contraction, it jumps to 2522 K at $t = 13$ μs due to the strong shock reflection from the left vertical plane. After the reflection, it decreases to 2377 K at $t = 13.7$ μs and then jumps to 3000 K due to the ignition at $t = 14$ μs. After the ignition, it fluctuates but still remains at a very high value. The spikes appearing after the ignition are caused by shock reflections and focusing. For the cases of 25 bar and 18 bar, as the incident shock reaches the left vertical wall, it increases to 1796 K at $t = 15.5$ μs and 1519 K at $t = 16.6$ μs respectively resulting in ignitions at $t = 16.3$ μs for the case of 25 bar and at $t = 17.7$ μs for the case of 18 bar. It is revealed that the temperature behind the reflected shock from the vertical wall decreases with release pressure. For the case of 25 bar, the maximum temperature stays well above 2000 K after the ignition indicating that the flames are sustained in the tube. While for the case of 18 bar the ignited flame is finally quenched at $t = 26$ μs and several spikes afterwards are also cause by shock focusing. To some extent this finding is consistent with Dryer et al.'s experimental observation in that the minimum release pressure for the release through a tube with internal geometries is only 20.4 bar [3].

5. Summary

The effect of a local contraction in the release tube on the spontaneous ignition of pressurized hydrogen release has been investigated. As the incident shock reaches the local contraction, a strong curvilinear reflected shock is generated receding towards the rupture plane. Swept by the reflected shock, the temperature of the flammable mixture at the contact region is elevated and reaches a maximum upstream the contraction where the first ignition kernel is initiated. The ignition kernels tend to quickly propagate along the contact interface and establish a partially premixed flame. The ignition kernel has a significant thickness in the mixture fraction space and the most reactive mixture fraction slightly deviates from that of the stoichiometric value.

The flow development at the contraction is very complicated due to shock formation, reflection and interaction. The curvilinear reflected shock from the left vertical wall converges and reflects from the axis of symmetry creating a high-speed jet flow inside the contraction. As the transmitted shock leaves the contraction, it diffracts into a curvilinear shock which is reflected from the tube wall. The reflected shock converges at the axis creating another high speed jet. As the leading shock wave propagates downstream the contraction section, a strong Mach disk gradually forms inside the underexpanded flow after the contraction while an annular supersonic flow develops along the tube wall. In addition to the repeating shock reflections between tube wall and the axis, these complex flow developments create a highly turbulent flow significantly distorting the contact region and enhancing its mixing. Although the ignition kernels are initiated at the thin contact region, partially premixed flames quickly develop due to the fast turbulent enhanced mixing. The partially premixed flames are highly distorted by the turbulent flow and overlapped with each other. Flame thickening was also observed due to the merge of thin flames.

According to the present study, the internal geometry of a local contraction can significantly facilitate the occurrence of spontaneous ignition by producing elevated flammable mixture and turbulent enhanced mixing. Accordingly, sustained flames are predicted for the release pressure as low as 25 bar, while quenched flames are predicted for the release pressure of 18 bar. To some extent this finding is consistent with Dryer et al.'s experimental observation in that the minimum release pressure for the release through a tube with internal geometries is only 20.4 bar [3].

Finally, only one type of internal geometry is presented in this paper due to the page limit although other three possible types of internal geometry i.e. a local expansion, a contraction followed by a constant diameter tube and an expansion followed by a constant diameter tube have also been numerically simulated by the authors. All types of internal geometry are found to increase the propensity to spontaneous ignition due to local shock reflection and focusing. However, shock reflection from a vertical wall has been found to result in a higher temperature than from a lateral wall. The findings suggest that care should be taken to avoid/reduce all types of internal geometry in order to reduce the propensity to hydrogen spontaneous ignition in pressurized release. These findings have practical implications for hydrogen safety as in practice there are often various fixtures inside the tubes.

REFERENCES

[1] Astbury GR, Hawksworth SH. Spontaneous ignition of hydrogen leaks: a review of postulated mechanisms. Int J Hydrogen Energy 2007;32:2178–85.
[2] Astbury GR. A review of the properties and hazards of some alternative fuels process safety and environmental protection. I Chem E 2008;86(6):397–414.
[3] Dryer FL, Chaos M, Zhao Z, Stein JN, Alpert JY, Homer CJ. Spontaneous ignition of pressurized releases of hydrogen and natural gas into air. Combust Sci Tech 2007;179:663–94.
[4] Mogi T, Kim D, Shiina H, Horiguchi S. Self-ignition and explosion during discharge of high-pressure hydrogen. J Loss Prevent Proc 2008;21:199–204.
[5] Golub VV, Baklanov DI, Bazhenova TV, Bragin MV, Golovastov SV, Ivanov MF, et al. Shock-induced ignition of

hydrogen gas during accidental or technical opening of high-pressure tanks. J Loss Prevent Proc 2008;21(2):185–98.
[6] Liu YF, Sato H, Tsuboi N, Hjigashino F, Hayashi AK. Numerical simulation on hydrogen fuel jetting from high pressure tank. Sci Tech Energ Mater 2006;67:7–11.
[7] Xu BP, Wen JX, Dembele S, Tam VHY, Hawksworth SJ. The effect of pressure boundary rupture rate on spontaneous ignition of pressurized hydrogen release. J Loss Prevent Proc 2009;22(3):279–87.
[8] Xu BP, EL Hima L, Wen JX, Tam VHY. Numerical study of spontaneous ignition of pressurized hydrogen release into air. Int J Hydrogen Energy 2009;34:5954–60.
[9] Yamada E, Watanabe S, Hayashi AK, Tsuboi N. Numerical analysis on autoignition of a high-pressure hydrogen jet spouting from a tube. Proc Combust Inst 2009;32(2):2363–9.
[10] Xu BP, EL Hima L, Wen JX, Dembele S, Tam VHY, Donchev T. Numerical study of spontaneous ignition of pressurized hydrogen release through a tube into air. J Loss Prevent Proc 2008;21(2):205–21.
[11] Wen JX, Xu BP, Tam VHY. Numerical study on spontaneous ignition of pressurized hydrogen release through a length of tube. Combust Flame 2009;156(11):2173–89.
[12] Xu BP, Wen JX, Tam VHY. The effect of an obstacle plate on the spontaneous ignition in pressurized hydrogen release: a numerical study. Int J Hydrogen Energy 2011;36(3):2637–44.
[13] Bragin MV, Molkov VV. Physics of spontaneous ignition of high-pressure hydrogen release and transition to jet fire. Int J Hydrogen Energy 2010;36(3):2589–96.
[14] Lee BJ, Jeung IS. Numerical study of spontaneous ignition of pressurized hydrogen released by the failure of a rupture disk into a tube. Int J Hydrogen Energy 2009;34:8763–9.
[15] Jiang GS, Shu CW. Efficient implementation of weighted ENO schemes. J Comput Phys 1996;126:202–28.
[16] Hirt CW, Amsden AA, Cook JL. An arbitrary Lagrangian-Eulerian computing method for all flow speeds. J Comput Phys 1974;14:227–53.
[17] Balsara DS, Shu CW. Monotonicity preserving WENO schemes with increasingly high-order of accuracy. J Comput Phys 2000;160:405–52.
[18] O'Rourke PJ, Amsden AA. Implementation of a conjugate residual iteration in the KIVA computer program. Los Alamos national laboratory report LA-10849-MS; 1986.
[19] Williams BA. Sensitivity of calculated extinction strain rate to molecular transport formulation in nonpremixed counterflow flames. Combust Flame 2001;124:330–3.
[20] Kee RJ, Rupley FA, Miller JA. Chemkin II: a fortran chemical kinetics package for the analysis of gas-phase chemical kinetics. Sandia national laboratories report no. SAND89–8009; 1989.
[21] Saxena P, Williams FA. Testing a small detailed chemical-kinetic mechanism for the combustion of hydrogen and carbon monoxide. Combust Flame 2006;145:316–23.
[22] Brown PN, Byrne GD, Hindmarsh AC. VODE, a variable-coefficient ODE solver, SIAM. J Sci Stat Comput 1989;10: 1038–51.
[23] Goozee RJ, Jacobs PA, Buttsworth DR. Simulation of complete reflected shock tunnel showing a vortex mechanism for flow contamination. Shock Waves 2006; 15(3–4):165–76.
[24] Jiang Z, Takayama K, Babinsky H, Meguro T. Transient shock wave flows in tubes with a sudden change in cross section. Shock Waves 1997;7:151–62.